Quantitative Analysis of Bacterial Gene Expression by Using the *gusA* Reporter Gene System

JUN SUN,[1] ILSE SMETS,[2] KRISTEL BERNAERTS,[2] JAN VAN IMPE,[2] JOS VANDERLEYDEN,[1]* AND KATHLEEN MARCHAL[3]

Centre of Microbial and Plant Genetics,[1] BioTeC-Bioprocess Technology and Control,[2] and SISTA, Department of Electrical Engineering,[3] Katholieke Universiteit Leuven, B-3001 Heverlee, Belgium

An *Azospirillum brasilense* Sp7 strain containing a plasmid-borne translational *cytN-gusA* fusion was grown in a continuous culture to quantitatively evaluate the influence of extracellular signals (such as O$_2$) on expression of the *cytNOQP* operon. The dissolved oxygen concentration was shifted at regular time intervals before the steady state was reached. The measured β-glucuronidase activity was used to monitor *cytN* gene expression. However, as the β-glucuronidase activity in the experimental setup not only depended on altered transcription of the hybrid gene when the signal was varied but was also influenced by cellular accumulation, degradation, and dilution of the hybrid fusion protein, a mathematical method was developed to describe the intrinsic properties of the dynamic bioprocess. After identification and validation of the mathematical model, the apparent specific rate of expression of the fusion, which was independent of the experimental setup, could be deduced from the model and used to quantify gene expression regulated by extracellular environmental signals. In principle, this approach can be generalized to assess the effects of external signals on bacterial gene expression.

Gene fusions containing reporter genes are widely used to monitor and quantify the effects of external signals on bacterial gene expression (11, 14). However, complications may arise if the external signals, such as the levels of O$_2$ and other substrates utilized by the bacteria, cannot be kept constant during the test (7). Since O$_2$ level is a very important external signal regulating expression of certain genes, a reliable method is needed to study the influence of O$_2$ on bacterial gene expression.

The use of a continuous culture in an O$_2$-stat to test the influence of O$_2$ on expression of a gene represents a major improvement in such studies (5, 12, 23, 24). In a continuous culture the O$_2$ concentration can be adjusted easily; thus, the effects of fluctuating cell densities and respiratory rates on O$_2$ concentrations can be compensated for. When the effects of constitutive O$_2$ shifts on gene expression are studied, measurements in a continuous fermentation are usually taken after establishment of a steady state (5, 12). Such experiments require extended fermentation times and therefore might involve a high risk of biological instability problems.

An experimental setup in which measurements could be taken after the O$_2$ shift occurs and before a steady state is reached would significantly enhance analysis. It should be noted that in such a setup the absolute expression level not only is dependent on altered transcription of the hybrid gene when the signal is varied but also is influenced by the cellular accumulation, degradation, and dilution rate of the hybrid fusion protein. (It should also be noted that even in a steady state, the absolute value for fusion protein activity depends on the implemented dilution rate and therefore is not completely independent of the experimental setup.) Therefore, a reliable method which is independent of the experimental parameters to describe the influence of O$_2$ on expression of genes can facilitate interpretation of the experimental data.

In this study, a method was developed to determine the mere influence of O$_2$ on expression of target genes. A general dynamic model was used to describe cell growth and fusion protein expression in a continuous culture in which the dissolved oxygen (DO$_2$) concentration was shifted at regular time intervals before the steady state was reached. The apparent specific rate of expression of the gene fusion, which was intrinsically independent of the experimental parameters, was defined and deduced from a validated mathematical model. The model was used to study induction of *cytN* gene expression by O$_2$ in *Azospirillum brasilense* Sp7 based on the activities of a *cytN-gusA* fusion. The *A. brasilense cytNOQP* operon, encoding a cytochrome *cbb*$_3$ terminal oxidase, has been shown to be involved in microaerobic growth and respiration (16). Model-based data analysis indicated that the optimal DO$_2$ level for expression of the *cytNOQP* genes is in the microaerobic range, which is consistent with a previous study (16).

MATERIALS AND METHODS

Plasmids, bacterial strains, and growth conditions. The strains and plasmids used in this study are listed in Table 1. Luria-Bertani medium was used for *Escherichia coli*, while MMAB medium (29) was used for *Azospirillum* strains. When required, ampicillin (100 μg/ml) or tetracycline (10 μg/ml) was added to the medium.

To construct the translational *cytN-gusA* fusion used in this study, a 517-bp upstream region of the *cytN* gene was PCR amplified and inserted into the *Pst*I-*Xba*I sites of plasmid pFAJ1171 (25) to generate plasmid pFAJ870. After

* Corresponding author. Mailing address: Centre of Microbial and Plant Genetics, K. U. Leuven, Kasteelpark Arenberg 20, B-3001 Heverlee, Belgium. Phone: 0032-16-321631. Fax: 0032-16-321966. E-mail: jozef.vanderleyden@agr.kuleuven.ac.be.

TABLE 1. Plasmids and bacterial strains used in this study

Plasmid or strain	Relevant characteristic(s)	Reference or source
pFAJ1171	pUC18 derivative containing the promoterless *gusA* gene from pBI101.3 on a 2-kb *Bam*HI-*Eco*RI fragment	25
pFAJ870	pFAJ1171 derivative containing a 517-bp fragment from the *cytN* gene of *A. brasilense* Sp7	This study
pFAJ873	pLAFR3 derivative containing a 2.6-kb *Pst*I-*Eco*RI fragment from pFAJ870	This study
pLAFR3	Broad-host-range vector, Tc^r	21
Azospirillum brasilense Sp7	Wild type (= ATCC 29145)	22
Escherichia coli DH5α	*hsdR17 endA1 thi-1 gyrA96 relA1 recA1 supE44 ΔlacU169* (Φ80*lacZ* ΔM15)	Gibco-BRL

verification by DNA sequence analysis, a 2.6-kb *Pst*I-*Eco*RI fragment from pFAJ870, containing the *cytN* upstream region fused to the promoterless *gusA* reporter gene, was cloned into the corresponding sites of plasmid pLAFR3 (21), yielding pFAJ873, which contained 427 bp of the *cytN* upstream region and the sequences encoding the first 29 amino acids of CytN fused to the GusA coding sequence. This plasmid was mobilized from *E. coli* DH5α to *A. brasilense* Sp7 by triparental conjugation.

Continuous fermentation was performed in a 2-liter O$_2$-stat fermentor as previously described (16) by using MMAB medium (29). The concentration of DO$_2$ was controlled by varying the air flow into the fermentor on the basis of the measured DO$_2$ value. Gaseous nitrogen was sparged into the fermentor at a flow rate of 1.27 liters/min at low DO$_2$ levels (0 to 15% DO$_2$).

Analytical procedures. Quantitative β-glucuronidase activity was measured as previously described (26); this activity was expressed in Miller units (17) but was calculated per hour instead of per minute. Cell growth was monitored by measuring the optical density at 578 nm (OD$_{578}$) with a Perkin-Elmer Lambda 2 UV spectrum spectrophotometer. The L-malate concentration in the culture broth was determined with a test kit from Boehringer (Mannheim, Germany). All data in this paper are averages based on at least two replicates.

Fermentation strategy. The bacteria were first cultivated in a batch fermentation. At the end of the exponential growth phase, continuous fermentation started. Consecutive small DO$_2$ concentration shifts were made before a new steady state was reached. The profiles of DO$_2$ concentrations during fermentation are shown in Fig. 1A, 2A, and 3A. Samples were taken about each 1.5 h (just

before a DO$_2$ concentration shift) and used to determine the β-glucuronidase activity and cell density. To monitor strain stability and purity, samples were collected at the end of the fermentation period and spread on indicator plates containing bromo-4-chloro-3-indolyl-β-glucuronide (X-Gluc) (11). During the continuous fermentation, the carbon source (malate) was designed to be the limiting factor.

Analysis of the fermentation data. Changes in the β-glucuronidase activity of a hybrid gene reporter in the presence of a changing external signal indicate that the external signal is the transcriptional activation signal. However, in the experimental setup described above, not only alterations in transcriptional activation of the plasmid encoding the *cytN-gusA* fusion induced by the DO$_2$ concentration shifts but also accumulation and turnover of the fusion protein can account for the β-glucuronidase activity measured. Therefore, only the specific rate of expression of the fusion protein, which is independent of the experimental design, can reflect the influence of O$_2$ on expression of the target gene. In order to derive the specific rate of expression of the fusion protein from the β-glucuronidase activity measured, the following general dynamic mathematical model based on mass balances was applied (28):

$$\frac{dX}{dt} = \mu X - DX \qquad (1)$$

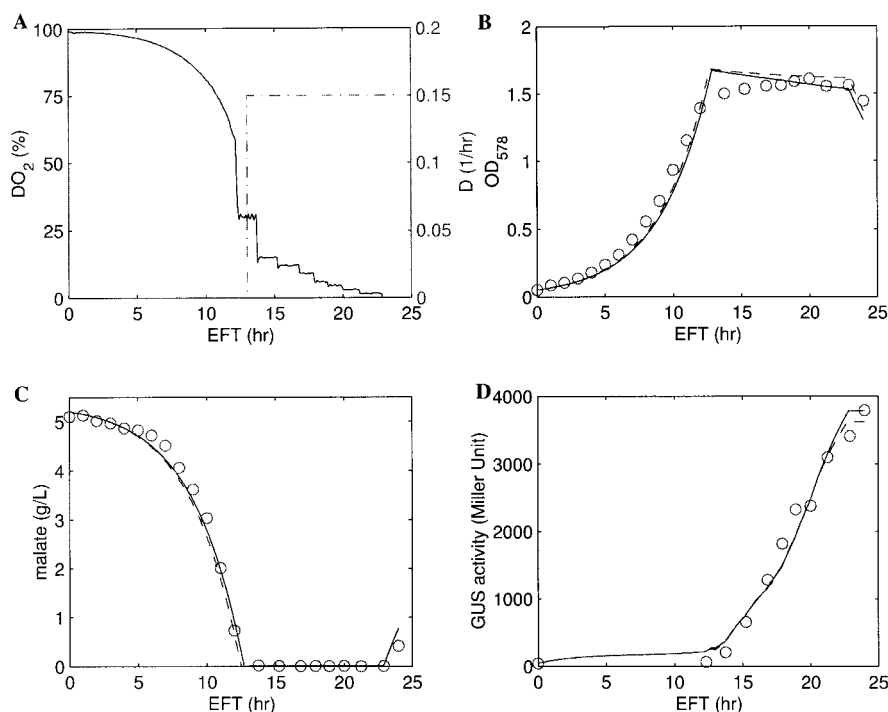$$\frac{dS}{dt} = -\sigma X - DS + DS_{in} \qquad (2)$$

FIG. 1. Identification of the mathematical model. (A) Profile of on-line-measured values for DO$_2$ concentration (DO$_2$) (solid line) and dilution rate (D) (dashed and dotted dot line). (B to D) ○, experimental data; solid line, simulation results obtained with the full model; dashed line, simulation results obtained with the simplified model. EFT, elapsed fermentation time; GUS, β-glucuronidase.
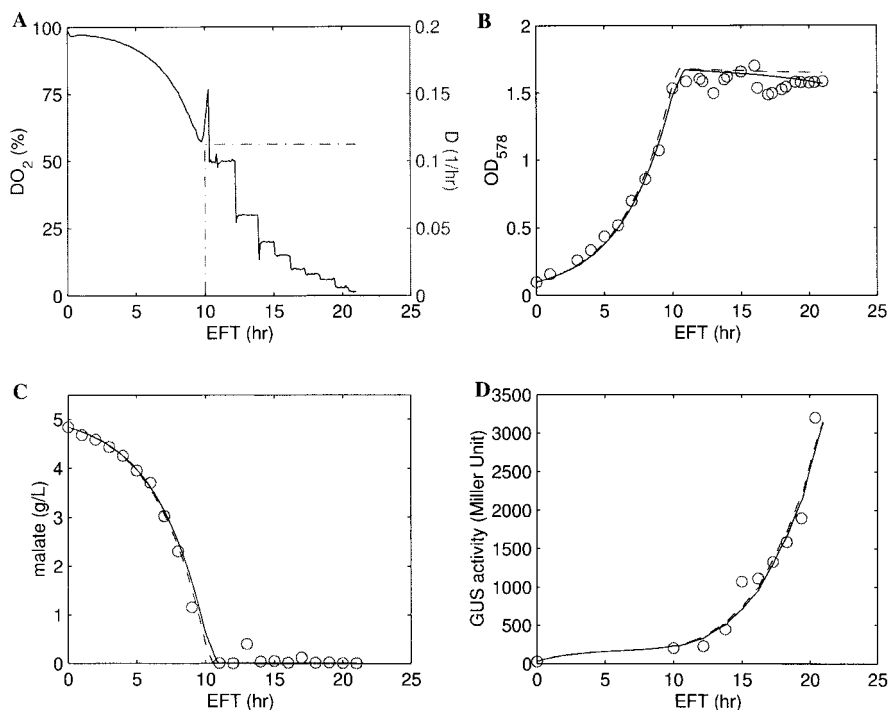
FIG. 2. Validation of the mathematical model. The symbols and abbreviations are the same as those described in the legend to Fig. 1.

$$\frac{dP}{dt} = \pi X - DP - kP \qquad (3)$$

where X is the concentration of biomass (grams of cells per liter), S is the concentration of the carbon source (grams of malate per liter), S_{in} is the concentration of the carbon source in the feed flow (grams of malate per liter), P is the concentration of the fusion protein (grams of protein per liter), D is the dilution rate (per hour),

μ is the specific growth rate of cells (per hour), σ is the specific rate of consumption of the carbon source (grams of malate per gram of cells per hour), π is the specific rate of expression of the fusion protein (grams of protein per gram of cells per hour), and k is the in vivo rate of degradation of the fusion protein (per hour).

According to the definition of β-glucuronidase activity (17), the β-glucuronidase activity value is assumed to be proportional to the amount of fusion protein per cell:
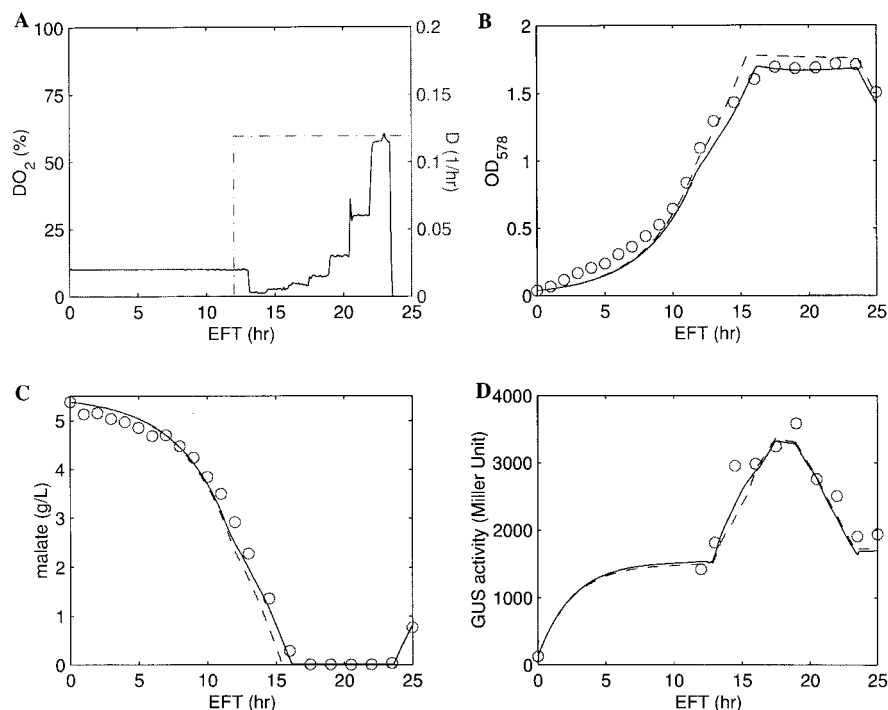

FIG. 3. Further validation of the mathematical model with a different DO_2 profile. The symbols and abbreviations are the same as those described in the legend to Fig. 1.

$$P = \alpha U X \qquad (4)$$

where U is the β-glucuronidase activity (Miller units [enzyme activity per gram of cells per hour]) and α is a proportionality constant (grams of protein per gram of cells per Miller unit).

By combining equation 4 with equations 1 and 3, the following equation can be deduced:

$$\frac{dU}{dt} = \beta - \mu U - kU \qquad (5)$$

where β is π/α (Miller units per hour), the apparent specific rate of expression of the fusion protein, and reflects the direct influence of the external signal on transcriptional activation of the hybrid gene fusion.

The three specific reaction rates can be correlated with equation 6:

$$\sigma = \frac{\mu}{Y_{XS}} + \frac{\beta}{Y_{US}} \qquad (6)$$

where Y_{XS} (grams of cells per gram of malate) and Y_{US} (Miller units per gram of cells) are two positive constant yield coefficients.

To complete the model, the following kinetic expressions are proposed. A double Haldane model is used to describe the specific growth rate of cells as a function of two substrates, malate and O_2 (1). The apparent specific rate of expression of the fusion protein is described as a function of the carbon substrate (malate) concentration with a Monod model (18) and as a function of DO_2 concentration with a Haldane-like model in which background expression of the fusion protein is introduced since constitutive background expression of the fusion protein has been observed under anaerobic conditions (data not shown). Although it is generally known that *E. coli* β-glucuronidase is a very stable enzyme in cell extracts and in cells (10, 11), no value for in vivo decay of any β-glucuronidase protein in *A. brasilense* has been described so far. However, the dependence of degradation of the fusion protein on DO_2 concentration has also been observed in experiments carried out in test tubes (data not shown). The rate of degradation of the fusion protein can be expressed as a function of DO_2 concentration in the frame of the Monod model (18). Therefore, the following equations are proposed:

$$\mu = \mu_{max} \cdot \frac{S}{(KM_{XS} + S + S^2/KI_{XS})} \cdot \frac{DO_2}{(KM_{XG} + DO_2 + DO_2^2/KI_{XG})} \qquad (7)$$

$$\beta = \beta_{max} \cdot \frac{S}{(KM_{PS} + S)} \cdot \frac{(DO_2 + KB_{PG})}{(KM_{PG} + DO_2 + DO_2^2/KI_{PG})} \qquad (8)$$

$$k = k_{max} \cdot \frac{DO_2}{(K_k + DO_2)} \qquad (9)$$

where DO_2 is the concentration of dissolved oxygen (percent); KM_{XS} and KI_{XS} are the saturation constant and inhibition constant of malate for cell growth (grams of malate per liter), respectively; KM_{XG} and KI_{XG} are the saturation constant and inhibition constant of DO_2 for cell growth (percent), respectively; KM_{PS} is the saturation constant of malate for fusion protein expression (grams of malate per liter); KM_{PG} and KI_{PG} are the saturation constant and inhibition constant of DO_2 for fusion protein expression (percent), respectively; KB_{PG} is the constant for background expression of the fusion protein (percent); K_k is the saturation constant of DO_2 for decay of the fusion protein (percent); μ_{max} is the maximal growth rate of cells (per hour); β_{max} is the maximal apparent rate of expression of the fusion protein (Miller units per hour); and k_{max} is the maximal rate of degradation of the fusion protein (per hour).

In order to assess the influence of DO_2 on the specific level of expression of the *cytN-gusA* fusion, the measured experimental values were fed into the model to identify the appropriate parameters. Once the values are identified, the complete model (parameters and model structure) can be used to predict the behavior of the hybrid fusion protein as a function of the external variables.

Simulation and parameter identification for the model described above were performed by using Matlab 5.3 (The MathWorks, Inc., Natick, Mass.) on a Linux platform.

RESULTS

Parameter identification. *A. brasilense* Sp7 containing plasmid pFAJ873 was cultivated in a fermentor for 13 h. Subsequently, continuous fermentation was started by maintaining the dilution rate at 0.15 h^{-1}. The DO_2 concentrations were

shifted before a steady state was reached at regular intervals (about 1.5 h). The profile of DO_2 concentration is shown in Fig. 1A. The parameters in the mathematical model were identified by minimizing the following cost function (*J*):

$$J = \sum_{j=1}^{n} \frac{\sum_{i=1}^{m} \left(\frac{Y_{s,ij} - Y_{e,ij}}{\bar{Y}_{e,ij}} \right)^2}{\sigma_{sj}^2} \qquad (10)$$

where i is the sampling time; j is the components X, S, and U; n ($n = 3$ in this case) and m are the number of components and the sampling time, respectively; $Y_{s,ij}$ is the data set for the simulation results; $Y_{e,ij}$ is the data set for the experimental results; $\bar{Y}_{e,j}$ is the average value for the components; and σ_{sj} is the standard deviation of the experimental data. In order to diminish the effects of the different physical quantities of the measurements, the relative errors, $(Y_{s,ij} - Y_{e,ij})/\bar{Y}_{e,j}$, are taken into account in cost function J.

The identification results are shown in Figure 1B to D, while the values for the identified parameters are summarized in Table 2. The estimated initial (zero-time) values were as follows: $S = 5.2087$ g of malate per liter; $X = 0.0554$ OD_{578} unit; and $U = 41.9123$ Miller units. The carbon source concentration in the feed flow (S_{in}) was 5.0075 g of malate per liter. Because cell density rather than dry weight of cells was used to monitor cell growth, the yield coefficient Y_{XS} as defined in equation 6 was expressed in OD_{578} units per gram of malate instead of grams of cells per gram of malate. The agreement between the simulation results and the experimental data is remarkable.

Validation of the mathematical model. To validate the model structure and parameters, an experimental test set was generated by performing a continuous fermentation similar to the one used for parameter identification but with a slightly different DO_2 profile (Fig. 2A) and different initial values. The continuous fermentation started at 10 h with a dilution rate of 0.1125 h^{-1}. The following initial values for validation were chosen from the first experimental measurements: $S = 4.8388$ g of malate per liter; $X = 0.097$ OD_{578} unit; and $U = 25.5267$ Miller units. For the carbon source concentrations in the feed flow, the following experimentally measured value was used: $S_{in} = 4.989$ g of malate per liter. Both the simulation results, as obtained by applying the model and parameters identified above, and the experimental data are shown in Fig. 2. The good agreement between the simulated and experimental results indicates the applicability of the model when comparable experimental conditions (such as DO_2 profile) are used.

In order to further validate the applicable range of the model, a continuous fermentation with a totally different DO_2 profile (Fig. 3A) was performed. The DO_2 concentration was kept at 10% during the batch fermentation, and it was subsequently shifted from low to high values during the continuous fermentation. The continuous fermentation started at 12 h with a dilution rate of 0.1193 h^{-1}. The following initial values used for validation were based on the first experimental measurements: $S = 5.3812$ g of malate per liter; $X = 0.038$ OD_{578} unit; and $U = 126.84$ Miller units. For the carbon source concentration in the feed flow, the following measured value was used: $S_{in} = 5.308$ g of malate per liter. The simulation results and the experimental data are shown in Fig. 3. The

TABLE 2. Summary of the parameters used in the general mathematical model

Parameter	Units	Description	Value
μ_{max}	Per hour	Maximal growth rate of cells	0.2785 h^{-1}
β_{max}	Miller units per hour	Maximal rate of expression of fusion protein	1.0387×10^4 Miller units/h
k_{max}	Per hour	Maximal rate of degradation of fusion protein	0.1270 h^{-1}
KM_{XS}	Grams of malate per liter	Saturation constant of malate for cell growth	1.58×10^{-2} g of malate/liter
KI_{XS}	Grams of malate per liter	Inhibition constant of malate for cell growth	7.805×10^3 g of malate/liter
KM_{XG}	Percent	Saturation constant of DO$_2$ for cell growth	0.1533%
KI_{XG}	Percent	Inhibition constant of DO$_2$ for cell growth	$6.1583 \times 10^3\%$
KM_{PS}	Grams of malate per liter	Saturation constant of malate for fusion protein expression	5.7782×10^{-4} g of malate/liter
KB_{PG}	Percent	Background expression constant of fusion protein	0.0056%
KM_{PG}	Percent	Saturation constant of DO$_2$ for fusion protein expression	7.6233%
KI_{PG}	Percent	Inhibition constant of DO$_2$ for fusion protein expression	0.6527%
K_k	Percent	Saturation constant of DO$_2$ for degradation of fusion protein	0.4781%
Y_{XS}	OD$_{578}$ units per gram of malate	Yield coefficient for biomass on carbon substrate	0.3282 OD$_{578}$ unit/g of malate
Y_{US}	Miller units per gram of malate	Yield coefficient for GUS activity on carbon substrate[a]	2.7181×10^4 Miller units/g of malate

[a] GUS, β-glucuronidase.

agreement between the simulated and experimental results corroborates the generality of the model.

Influence of O$_2$ on the rate of expression of the target genes. As indicated in Fig. 4A and B, the rate of expression of the *cytN-gusA* fusion is very dependent on the DO$_2$ concentration, and the maximal values occur under microaerobic conditions (a DO$_2$ concentration of 2.23% results in maximal expression).

As shown by the values for KM_{XG} and KI_{XG} in Table 2, the model predicts that O$_2$ is not a limiting factor for cell growth under the conditions tested. In view of the highly efficient

microaerobic metabolism of *Azospirillum* (30), such behavior is not unexpected. The minor effect of carbon substrate concentration on the apparent specific rate of expression is also predicted by the model, implying that the *cytNOQP* operon is not subject to catabolic repression by malate. Furthermore, the specific rate of degradation of the fusion protein as a function of the DO$_2$ concentration is shown in Fig. 4C. The maximal specific rate of degradation of the fusion protein is 0.1270 h^{-1}, corresponding to a half-life of 5.46 h. The native CytN protein is a transmembrane protein (16), but its GusA fusion counter-
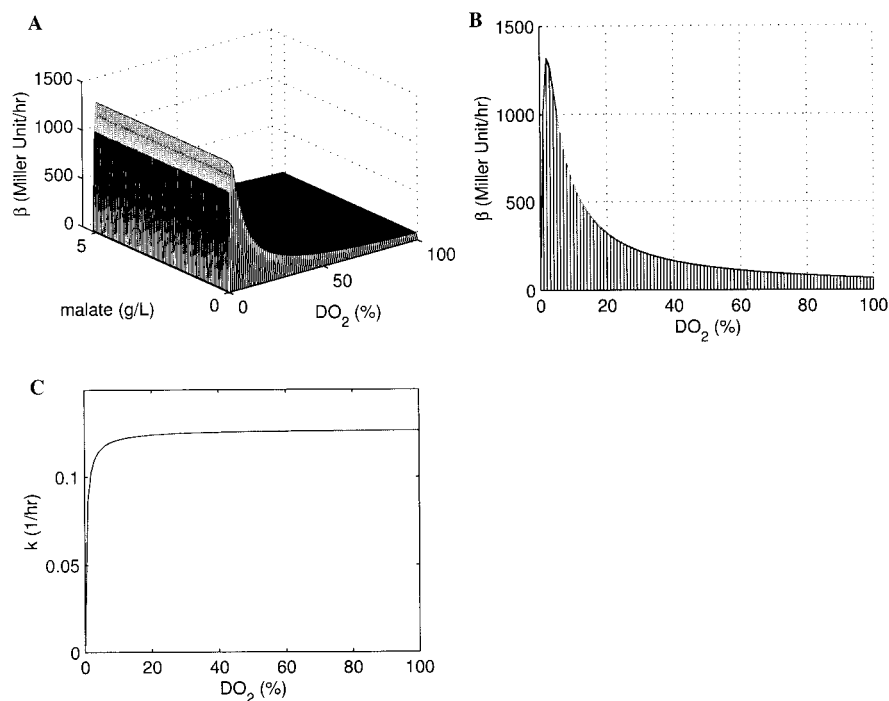

FIG. 4. (A) Apparent specific rate of expression of fusion protein as a function of the concentrations of the substrates malate and DO$_2$. (B) Cross section of panel A at a constant malate concentration of 1 g/liter. (C) Specific rate of degradation of fusion protein as a function of DO$_2$ concentration.

TABLE 3. Summary of the parameters used in the simplified mathematical model

Parameter	Units	Description	Value
μ_{max}	Per hour	Maximal growth rate of cells	$0.2785\ h^{-1}$
β_{max}	Miller units per hour	Maximal rate of expression of fusion protein	1.0387×10^4 Miller units/h
k_{max}	Per hour	Maximal rate of degradation of fusion protein	$0.1270\ h^{-1}$
KM_{PG}	Percent	Saturation constant of DO_2 for fusion protein expression	7.6233%
KI_{PG}	Percent	Inhibition constant of DO_2 for fusion protein expression	0.6527%
Y_{XS}	OD_{578} units per gram of malate	Yield coefficient for biomass on carbon substrate	$0.3282\ OD_{578}$ unit/g of malate
ε_1		Constant	10^{-2}
ε_2		Constant	10^{-6}

part lacks any potential transmembrane region and should therefore be cytoplasmically located. The cytoplasmic GusA fusion appears to be a stable protein in *A. brasilense*.

Towards a simplified model. When the general model structure represented by equations 1, 2, 5, and 6 to 9 is examined and the large range of orders of magnitude for the 14 parameters summarized in Table 2 is considered, a legitimate question is whether a similar high-quality fit of the experimental data can be obtained with a simplified model that includes fewer parameters. In order to mathematically investigate this possibility, a thorough sensitivity analysis was performed.

The dilution rate and the DO_2 concentration were defined as system inputs u_1 and u_2, respectively, and the biomass concentration, the malate concentration, and the β-glucuronidase activity were defined as system outputs y_1, y_2, and y_3, respectively. The parameters were denoted p_j with j ranging from 1 to 14.

A 3×14 sensitivity matrix containing the sensitivity functions $(\partial y_i/\partial p_j)(t)$ was then computed. These sensitivity functions represent the sensitivity of each output (y_i) to (small) variations in each model parameter (p_j). More details on sensitivity function-related procedures have been described by Bernaerts et al. (3).

Based on the sensitivity functions and the experimental data, the kinetic expressions (equations 7 to 9) of the general model described above could be substantially simplified as follows:

$$\mu = \mu_{max} \cdot \frac{S}{(\varepsilon_1 + S)} \cdot \frac{DO_2}{(\varepsilon_2 + DO_2)} \tag{11}$$

$$\beta = \beta_{max} \cdot \frac{S}{(\varepsilon_2 + S)} \cdot \frac{DO_2}{(KM_{PG} + DO_2 + DO_2^2/KI_{PG})} \tag{12}$$

$$k = k_{max} \cdot \frac{DO_2}{(\varepsilon_2 + DO_2)} \tag{13}$$

Meanwhile, the correlation among the three specific reaction rates can be simplified as equation 14:

$$\sigma = \frac{\mu}{Y_{XS}} \tag{14}$$

The number of model parameters has been reduced to six. The parameters and constants in the simplified kinetic expressions (equations 11 to 13) are summarized in Table 3.

As Table 3 and equations 11 to 14 show, most of the saturation constants are replaced by ε_1 or ε_2. The former is the same order of magnitude as the residual substrate concentration (i.e., 10^{-2}) and results in a 50% reduction in the specific growth rate when the malate concentration is low. The latter is a very small number (e.g., 10^{-6}) and results in a switch from the maximum specific rate when substrate or DO_2 is present to a rate of zero when both substrates are absent. Furthermore, the inhibition constants (i.e., KI_{XS} and KI_{XG}) that have been omitted can be considered replaced by an infinitely large (positive) number corresponding to a noninhibition situation. Note, however, that from a mechanistic point of view, it cannot be claimed that growth of *A. brasilense* is not inhibited by high substrate or DO_2 concentrations. We merely concluded that an inhibition effect cannot be inferred from the available experimental data. Also, the yield coefficient Y_{US} is assumed to be infinitely large to reflect the negligible contribution of product formation to the substrate consumption rate.

Figure 1 (identification) and Fig. 2 and 3 (validation) illustrate that the descriptive quality of this simplified model is as good as the descriptive quality of the original 14-parameter model. Note that there was apparently no need to reoptimize the six parameters in the simplified model (Tables 2 and 3).

Detailed exploration of the significance of model parameters in the general model, as well as in the simplified model, is the subject of ongoing research. Thus, optimal experiments (complemented with parameter uncertainty analysis) will be designed to check whether the model features present in the general model but omitted in the simplified model (e.g., inhibition of the specific growth rate at high substrate or DO_2 concentrations, the presence of background gene expression in the absence of DO_2) are truly needed.

DISCUSSION

Use of a dynamic mathematical model allows reliable quantitative interpretation of gene expression measurements as a function of varying environmental conditions without a requirement for a steady state. The parameters of the model are determined by using experimental data. When validated, the model can be used to predict in silico the effects of external signals on expression of the gene studied under nonexperimentally tested conditions. The use of mathematical models based on differential equations to describe and predict the behavior of cellular processes is becoming widespread (4, 6, 8, 9, 13, 20, 27). According to previous studies with *E. coli*, a steady state can be achieved within 5 reactor residence times (12, 23, 24), which equals 33 h at a dilution rate of $0.15\ h^{-1}$. A total fermentation time of 297 h (12 days) would be needed to test nine different DO_2 levels. The overall experimental time can be decreased to only 15 h when the DO_2 level is varied each 1.5 h and a mathematical model is used to analyze the results;

this yields more detailed information about the effects of external signals on expression of the genes.

In this study, a mathematical model was used to predict the specific pattern of expression of an *A. brasilense cytN-gusA* fusion as a function of DO_2 concentration. The role of the *cytNOQP*-encoded oxidase during microaerobic respiration and the presence of an FNR-binding consensus sequence in the upstream region of the *A. brasilense cytN* gene (16) point towards microaerobic regulation of the operon by an FNR-like protein. The simulated behavior of the *A. brasilense* hybrid *cytN-gusA* fusion, showing clear upregulation under microaerobic conditions, was therefore in good agreement with results obtained previously for the *A. brasilense* cytochrome cbb_3 oxidase. Moreover, it is noteworthy that the DO_2 concentration that resulted in maximal specific expression of the *cytN-gusA* fusion was approximately the same as the DO_2 concentration reported by Zhulin et al. (30) and coincided with generation of a maximal proton motive force. Furthermore, an expression pattern similar to the one obtained in this study has been reported for the CytN-like protein of *Rhodobacter sphaeroides* (19).

The model assumes that the shift in expression of the target gene occurs as soon as the DO_2 shift occurs. However, we cannot exclude the possibility that there may be a lag between signal transduction and fusion protein synthesis (for example, the delay between maximal mRNA synthesis and maximal protein synthesis). Usually, such a delay in prokaryotes is minimal (15). If a longer response time is expected (2), it is advisable to adapt the time intervals for measurements accordingly. Thus, the effects caused by the transition are similar for different DO_2 levels, and the results are comparable.

On the basis of a careful sensitivity analysis, a simplified model (with fewer parameters) was deduced in this case study, and this model had predictive values similar to those of the full model. The key feature of both the full model and the simplified model is mathematical description of fusion protein biosynthesis and degradation during bacterial growth. Given the high predictive value of these models, it is sensible to assume that they can form a basis for evaluating the effects of other external environmental signals, such as nitrogen source or other substrates which can be utilized by bacteria, on expression of target genes by using suitable fusions with the appropriate reporter genes. In view of fermentation technology, when optimization of heterologous gene expression is desired, such studies might allow workers to determine the environmental conditions that result in maximal gene expression.

REFERENCES

1. **Andrews, J. F.** 1968. A mathematical model for the continuous culture of microorganisms utilizing inhibiting substrates. Biotechnol. Bioeng. **10:**707–723.
2. **Baumann, B., M. Snozzi, A. J. B. Zehnder, and J. R. van der Meer.** 1996. Dynamics of denitrification activity of *Paracoccus denitrificans* in continuous culture during aerobic-anaerobic changes. J. Bacteriol. **178:**4367–4374.
3. **Bernaerts, K., K. J. Versyck, and J. F. Van Impe.** 2000. On the design of optimal dynamic experiments for parameter estimation of a Ratkowsky-type growth kinetics at suboptimal temperatures. Int. J. Food Microbiol. **54:**27–38.
4. **Cain, S. J., and P. C. Chau.** 1998. Transition probability cell cycle model with product formation. Biotechnol. Bioeng. **58:**387–394.
5. **Chao, G., J. Shen, C. P. Tseng, S.-J. Park, and R. P. Gunsalus.** 1997. Aerobic regulation of isocitrate dehydrogenase gene (*icd*) expression in *Escherichia coli* by the *arcA* and *fnr* gene products. J. Bacteriol. **179:**4299–4304.
6. **Chen, T., H. L. He, and G. M. Church.** 1999. Modeling gene expression with differential equations, p. 29–40. *In* R. B. Altman (ed.), The Pacific Symposium of Biocomputing '99, World Scientific, Hawaii.
7. **Cotter, P. A., and R. P. Gunsalus.** 1992. Contribution of the *fnr* and *arcA* gene products in coordinate regulation of cytochrome o and d oxidase (*cyoABCDE* and *cydAB*) genes in *Escherichia coli*. FEMS Microbiol. Lett. **91:**31–36.
8. **Goldbeter, A.** 1991. A minimal cascade model for the mitotic oscillator involving cyclin and cdc2 kinase. Proc. Natl. Acad. Sci. USA **88:**9107–9111.
9. **Goldbeter, A., G. Dupont, and M. J. Berridge.** 1990. Minimal model for signal-induced Ca^{2+} oscillations and for their frequency encoding through protein phosphorylation. Proc. Natl. Acad. Sci. USA **87:**1461–1465.
10. **Jefferson, R. A., S. M. Burgess, and D. Hirsh.** 1986. β-Glucuronidase from *Escherichia coli* as a gene-fusion marker. Proc. Natl. Acad. Sci. USA **83:**8447–8451.
11. **Jefferson, R. A., T. A. Kavanagh, and M. W. Bevan.** 1987. GUS fusions: β-glucuronidase as a sensitive and versatile gene fusion marker in higher plants. EMBO J. **6:**3901–3907.
12. **Kasimoglu, E., S.-J. Park, J. Malek, C. P. Tseng, and R. P. Gunsalus.** 1996. Transcriptional regulation of the proton-translocating ATPase (*atpIBEF HAGDC*) operon of *Escherichia coli*: control by cell growth. J. Bacteriol. **178:**5563–5567.
13. **Koh, B.-T., R. B. H. Tan, and M. G. S. Yap.** 1998. Genetically structured mathematical modeling of *trp* attenuator mechanism. Biotechnol. Bioeng. **58:**502–509.
14. **Lambrecht, M., A. Vande Broek, and J. Vanderleyden.** 1999. The use of GUS reporter system to study molecular aspects of interactions between bacteria and plants, p. 87–97. *In* J. Jansson (ed.), Tracking genetically engineering microorganisms: method development from microcosms to the field. RG Landes Bioscience, Georgetown, Tex.
15. **Lodish, H., D. Baltimore, A. Berk, S. L. Zipursky, P. Matsudaira, and J. Darnell.** 1995. Molecular cell biology, p. 406–407. Scientific American Books, Inc., New York, N.Y.
16. **Marchal, K., J. Sun, V. Keijers, H. Haaker, and J. Vanderleyden.** 1998. A cytochrome cbb_3 (cytochrome c) terminal oxidase in *Azospirillum brasilense* Sp7 supports microaerobic growth. J. Bacteriol. **180:**5689–5696.
17. **Miller, J. H.** 1972. Experiments in molecular genetics, p. 354–358. Cold Spring Harbor Laboratory, Cold Spring Harbor, N.Y.
18. **Monod, J.** 1942. Recherches sur la croissance des cultures bactériennes. Hermann, Paris, France.
19. **Mouncey, N. J., and S. Kaplan.** 1998. Oxygen regulation of the *ccoN* gene encoding a component of the cbb_3 oxidase in *Rhodobacter sphaeroides* 2.4.1T: involvement of the FnrL protein. J. Bacteriol. **180:**2228–2231.
20. **Novak, B., and J. J. Tyson.** 1997. Modeling the control of DNA replication in fission yeast. Proc. Natl. Acad. Sci. USA **94:**9147–9152.
21. **Staskawicz, B., D. Dahlbeck, N. Keen, and C. Napoli.** 1987. Molecular characterization of cloned avirulence genes from race 0 and race 1 of *Pseudomonas syringae* pv. *glycinea*. J. Bacteriol. **169:**5789–5794.
22. **Tarrand, J. J., N. R. Krieg, and J. Döbereiner.** 1978. A taxonomic study of the *Spirillum lipoferum* group, with description of a new genus, *Azospirillum* gen. nov., and two species, *Azospirillum lipoferum* (Beijerinck) comb. nov. and *Azospirillum brasilense* sp. nov. Can. J. Microbiol. **24:**967–980.
23. **Tseng, C.-P., J. Albrecht, and R. P. Gunsalus.** 1996. Effect of microaerophilic cell growth conditions on expression of the aerobic (*cyoABCDE* and *cydAB*) and anaerobic (*narGHJI, frdABCD,* and *dmsABC*) respiratory pathway genes in *Escherichia coli*. J. Bacteriol. **178:**1094–1098.
24. **Tseng, C.-P., A. K. Hansen, P. Cotter, and R. P. Gunsalus.** 1994. Effect of cell growth rate on expression of the anaerobic respiratory pathway operons *frdABCD, dmsABC,* and *narGJJI* of *Escherichia coli*. J. Bacteriol. **176:**6599–6605.
25. **Vande Broek, A.** 1994. Histochemical and genetic analysis of the *A. brasilense* -plant root association. Ph.D. thesis. Katholieke Universiteit Leuven, Heverlee, Belgium.
26. **Vande Broek, A., J. Michiels, S. M. de Faria, A. Milcamps, and J. Vander-**

leyden. 1992. Transcription of the *Azospirillum brasilense nifH* gene is positively regulated by NifA and NtrA and is negatively controlled by the cellular nitrogen status. Mol. Gen. Genet. **232:**592–600.

27. **Van Dien, A. J., and J. D. Keasling.** 1998. A dynamic model of the *Escherichia coli* phosphate-starvation response. J. Theor. Biol. **190:**37–49.

28. **Van Impe, J. F., and G. Bastin.** 1995. Optimal adaptive control of fed-batch fermentation processes. Control Eng. Practice **3:**939–954.

29. **Vanstockem, M., K. Michiels, J. Vanderleyden, and A. Van Gool.** 1987. Transposon mutagenesis of *Azospirillum brasilense* and *Azospirillum lipoferum*: physical analysis of Tn5 and Tn5-mob insertion mutants. Appl. Environ. Microbiol. **53:**410–415.

30. **Zhulin, I. B., V. A. Bespalov, M. S. Johnson, and B. L. Taylor.** 1996. Oxygen taxis and proton motive force in *Azospirillum brasilense.* J. Bacteriol. **178:**5199–5204.